Washington University School of Medicine
Digital Commons@Becker

Open Access Publications

2016

Microstructural and mechanical properties of the posterior cruciate ligament: A comparison of the anterolateral and posteromedial bundles

Jon O. Wright
Washington University School of Medicine in St. Louis

Nathan W. Skelley
Washington University School of Medicine in St. Louis

Reid P. Schur
Washington University in St. Louis

Ryan M. Castile
Washington University in St. Louis

Spencer P. Lake
Washington University School of Medicine in St. Louis

See next page for additional authors

Follow this and additional works at: https://digitalcommons.wustl.edu/open_access_pubs

Authors

Jon O. Wright, Nathan W. Skelley, Reid P. Schur, Ryan M. Castile, Spencer P. Lake, and Robert H. Brophy

Microstructural and Mechanical Properties of the Posterior Cruciate Ligament

A Comparison of the Anterolateral and Posteromedial Bundles

Jon O. Wright, MD, Nathan W. Skelley, MD, Reid P. Schur, BS, Ryan M. Castile, BS, Spencer P. Lake, PhD, and Robert H. Brophy, MD

Investigation performed at Washington University in St. Louis, St. Louis, Missouri

Background: The microstructural organization (collagen fiber alignment) of the posterior cruciate ligament (PCL), which likely corresponds with its functional properties, has only been described qualitatively in the literature, to our knowledge. The goal of this study was to quantify the tensile mechanical and microstructural properties of the PCL and compare these qualities between the anterolateral and posteromedial bundles.

Methods: Twenty-two knee specimens from 13 donors (8 male and 5 female; mean age [and standard deviation] at the time of death, 43.0 ± 4.1 years; mean body mass index, 30.0 ± 6.7 kg/m^2) were dissected to isolate the PCL, and each bundle was split into 3 regions. Mechanical testing of each regional sample consisted of preconditioning followed by a ramp-and-hold stress-relaxation test and a quasi-static ramp-to-failure test. Microstructural analysis was performed with use of a high-resolution, division-of-focal-plane polarization camera to evaluate the average direction of collagen orientation and the degree to which the collagen fibers were aligned in that direction. Results were compared between the anterolateral and posteromedial bundles and across the regions of each bundle.

Results: The anterolateral and posteromedial bundles demonstrated largely equivalent mechanical and microstructural properties. Elastic moduli in the toe and linear regions were not different; however, the posteromedial bundle did show significantly more stress relaxation ($p = 0.004$). There were also few differences in microstructural properties between bundles, which again were seen only in stress relaxation. Comparing regions within each bundle, several mechanical and microstructural parameters showed significant relationships across the posteromedial bundle, following a gradient of decreasing strength and alignment from anterior to posterior.

Conclusions: The PCL has relatively homogenous microstructural and mechanical properties, with few differences between the anterolateral and posteromedial bundles. This finding suggests that distinct functions of the PCL bundles result primarily from size and anatomical location rather than from differences in these properties.

Clinical Relevance: These properties of the PCL can be used to assess the utility of graft choices and operative techniques for PCL reconstruction and may partly explain limited differences in the outcomes of single-bundle compared with double-bundle reconstruction techniques for the PCL.

The posterior cruciate ligament (PCL) is the primary restraint to posterior translation of the tibia relative to the femur[1-3] and is composed of 2 bundles: the anterolateral and the posteromedial[2,4-6]. Considerable research has been dedicated to investigating PCL anatomy and function, as PCL disruptions can be associated with knee instability and altered knee kinematics[7-11].

While a large proportion of PCL injuries can be treated nonoperatively[12-17], high-grade isolated PCL injuries and multiligament knee injuries may be treated operatively with reconstruction[11,17-20] or, less commonly, repair[9,21-23]. Previous research characterizing the mechanical properties of the PCL has been limited by sample-preparation techniques, imaging technology, and the understanding of tissue mechanics at the

TABLE I Donor Demographics							
Donor	Age at Death *(yr)*	Sex	Height *(cm)*	Mass *(kg)*	BMI *(kg/m²)*	Cause of Death	Side*
1	45	F	173	128.0	42.9	Pulmonary embolism	R, L
2	45	M	188	134.4	38.0	Myocardial infarction	R, L
3	45	F	168	77.1	27.4	Anoxia	R, L
4	46	M	188	66.5	18.8	Self-inflicted gunshot wound	L
5	38	M	178	79.6	25.2	Heroin overdose	R, L
6	37	F	163	90.0	34.0	Intracranial bleed	R, L
7	48	F	165	82.2	26.8	Anoxia	L
8	41	M	180	94.0	28.9	Myocardial infarction	R, L
9	46	F	165	62.0	22.7	Myocardial infarction	R
10	48	M	173	95.9	32.1	Heart disease	R, L
11	36	M	175	88.0	28.6	Myocardial infarction	R, L
12	41	M	175	82.9	27.0	Natural causes	L
13	43	M	175	115.9	37.7	Anoxia	R, L

*When possible, both knees from each donor were tested.

time[24-27]. In addition, the microstructural organization (collagen fiber alignment) of the PCL, which likely corresponds with its functional properties, has only been described qualitatively in the literature, to our knowledge[25].

The purpose of the present study was to quantify the tensile mechanical and microstructural properties of the PCL bundles under dynamic tensile loading. We used a novel polarization imaging technique to allow for real-time analysis of collagen fiber alignment during mechanical testing. On the basis of previous findings in both the anterior cruciate ligament (ACL)[28,29] and the PCL[27,30], we hypothesized that the anterolateral and posteromedial bundles would exhibit distinct mechanical and microstructural properties.

Materials and Methods

Study Design

Human cadaveric tissues were handled in accordance with the Washington University School of Medicine in St. Louis body-donation policy. Institutional review board approval was not needed for the cadaveric study design. Inclusion criteria consisted of cadavers from patients who were <55 years of age at the time of death and had a body mass index (BMI) of <43 kg/m². Exclusion criteria consisted of knee samples with a history of trauma, surgery, or instability as well as those from patients with recorded genetic conditions that could affect bone or ligament composition. Power analysis demonstrated that 14 PCLs (a total of 84 regional samples) would be required to avoid a type-II error with β = 0.20 and α = 0.05.

Harvest Technique

Twenty-two knee specimens from 13 donors (8 male and 5 female; mean age [and standard deviation] at the time of death, 43.0 ± 4.1 years; mean BMI, 30.0 ± 6.7 kg/m²) fitting the selection criteria were acquired (Table I). Ligament tissues were kept hydrated with phosphate-buffered saline (PBS) solution during all stages of this study, including dissection, sample preparation, and mechanical testing.

Soft tissues were removed, leaving only the ACL, PCL, menisci, and meniscofemoral ligaments intact. An oscillating saw was used to split the femoral condyles, starting in the trochlear groove. The split was completed near the PCL and ACL attachments with use of an osteotome for better control, preserving the osseous attachments of the PCL in order to maintain proper ligament orientation. After the condyles were separated, the synovium was removed to differentiate the PCL from the anterior and posterior meniscofemoral ligaments. The meniscofemoral ligaments, when present, were carefully

Fig. 1
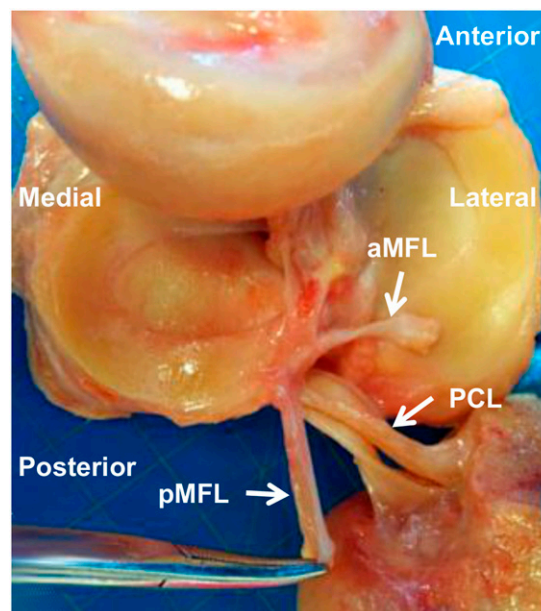
Photograph of a sample dissection, with a superior view looking down onto the tibial plateau with the femoral condyles rotated to show the PCL. The anterior and posterior meniscofemoral ligaments (aMFL and pMFL) are identified and separated from the PCL. The PCL is subsequently divided into anterolateral and posteromedial bundles before being further split into 3 coronal sections per bundle.
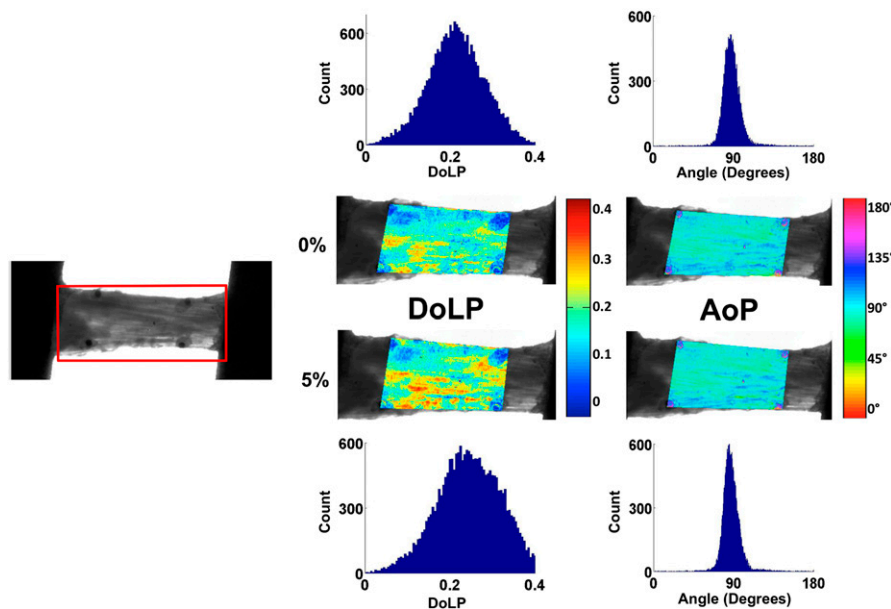
Fig. 2

Left: Grayscale image of a representative sample shows the markers used for strain tracking and for defining the polarization imaging region of interest. *Center and right:* Corresponding DoLP and AoP heat maps are shown at 0% and 5% strain with corresponding pixel-count histograms. At 5% strain, a shift to larger DoLP values and a narrowing of the AoP histogram are evident, demonstrating increased alignment compared with the sample at 0% strain.

dissected from the PCL and sharply dissected from their femoral attachments (Fig. 1). In 6 knees, an oblique fascicle of fibers was noted just posterior to the bulk of the posteromedial bundle, as described in a previous anatomical study[4]. Since these fascicles were too small for testing, they were discarded.

The division between the bundles of the PCL was identified on the basis of previous descriptions of PCL structural orientation, anatomical landmarks, and the behavior of each bundle under joint flexion and extension[2-4,6,31]. The division was bluntly developed at the femoral attachments, and then it was bluntly extended down to the tibial attachments. Once the bundles were separated, 2 incisions were made in each bundle in the coronal plane, just inferior to the femoral insertion, and they were extended down to divide each bundle into 3 regions. Each region was then marked at the lateral aspect of the femoral insertion to maintain orientation throughout testing and was detached from bone.

The 6 regions were numbered by anteroposterior orientation: region 1 (most anterior) through region 6 (most posterior), with regions 1 to 3 composing the anterolateral bundle and regions 4 to 6 composing the

posteromedial bundle. The regions were thinned into approximately 600-μm regional samples with use of a freezing-stage sliding microtome. Cross-sectional area was measured with use of a 3-dimensional (3D) laser scanning system and a custom MATLAB program (The MathWorks), and the mean cross-sectional area of each regional sample was recorded for subsequent stress calculations.

Sample Testing

Each regional sample was harvested, and the ends were affixed to small pieces of sandpaper using cyanoacrylate. Four 0.5-mm-diameter brass beads (Small Parts) were attached with cyanoacrylate to the central portion of each sample to provide points of reference for strain tracking and microstructural analysis.

Testing was performed with use of a tensile testing machine (TestResources). The sandpaper ends of the samples were placed in custom aluminum clamps with corresponding sandpaper footings to provide the necessary force transference without compressing or compromising the tissue itself, and the clamps were then attached to the actuators of the testing machine. The mechanical
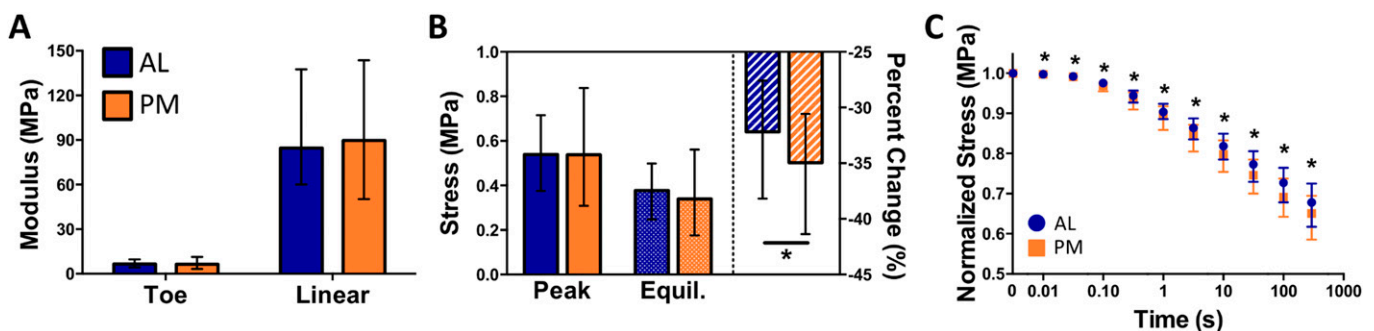
Fig. 3

Mechanical properties by bundle. **Fig. 3-A** Elastic moduli in the toe and linear regions of the stress-strain diagram of the quasi-static ramp-to-failure test. **Fig. 3-B** Stress at peak and equilibrium as well as percent relaxation during the stress-relaxation test. **Fig. 3-C** Rate of relaxation; normalized stress at each time point of the stress-relaxation test showing significant differences between bundles at all time points, including the first. The asterisks indicate significance ($p < 0.05$); bars indicate the median, and error bars indicate the 75th and 25th percentiles; AL = anterolateral, PM = posteromedial, and Equil. = equilibrium.

TABLE II Statistical Results Comparing Mechanical and Microstructural Properties of the PCL*							
	Between Bundles P Value	Across Anterolateral Regions (1 to 3)			Across Posteromedial Regions (4 to 6)		
		R^2	Slope	P Value	R^2	Slope	P Value
Mechanics							
Toe modulus	0.278	0.625	−0.324	0.519	0.489	−0.875	0.326
Linear modulus	0.059	<0.001	−9.347	0.284	<0.001	−25.340	0.042†
Transition stress	0.669	<0.001	−0.011	0.710	0.338	−0.058	0.124
Transition strain	0.232	0.590	0.000	0.952	0.350	−0.001	0.759
Peak stress	0.475	0.326	−0.041	0.357	<0.001	−0.109	0.043†
Equilibrium stress	0.767	0.329	−0.032	0.333	<0.001	−0.080	0.037†
Percent relaxation	0.004†	0.420	1.081	0.138	0.015	1.503	0.127
Microstructure							
Mean DoLP							
Zero	0.152	0.399	−0.011	0.129	<0.001	−0.016	0.020†
Transition	0.416	0.466	−0.013	0.126	0.319	−0.037	<0.001†
Linear	1.000	0.506	−0.010	0.228	0.349	−0.041	<0.0001†
Peak	0.894	0.527	−0.012	0.171	0.656	−0.038	<0.001†
Equilibrium	0.683	0.503	−0.013	0.142	0.627	−0.037	<0.001†
Percent change	0.096	0.579	0.124	0.814	0.118	−0.129	0.841
AoP standard deviation							
Zero	0.187	0.338	0.727	0.195	<0.001	2.452	<0.001†
Transition	0.512	0.263	0.695	0.149	0.133	2.961	<0.0001†
Linear	0.788	0.373	0.627	0.155	0.110	3.038	<0.0001†
Peak	0.018†	0.521	0.660	0.249	0.059	3.253	<0.0001†
Equilibrium	0.018†	0.535	0.696	0.242	<0.001	3.116	<0.0001†
Percent change	0.009†	0.503	0.172	0.808	0.051	2.193	0.032†

*Analyses were performed to compare properties between bundles as well as properties across the 3 subregions of each bundle. P values are provided for the results from each linear mixed-model analysis; r^2 coefficients, slope, and p values are provided for each linear regression of regional data. †A p value of <0.05 was considered significant.

testing system was integrated with a custom-built quantitative polarized light imaging system that consisted of a fiber optic backlight (Dolan-Jenner); a circularly polarizing film (Dolan-Jenner); and a high-resolution, division-of-focal-plane polarization camera[32,33].

Ligament samples were preloaded to 0.1 N to remove slack, and specimen gauge length was measured before each sample was tested. Testing consisted of 10 cycles of preconditioning by stretching the samples from 1.5% to 4.5% strain, a ramp-and-hold stress-relaxation test (a 5% strain step and dwell time of 300 seconds), and a quasi-static ramp-to-failure test at a strain rate of 1% per second. Images were acquired at approximately 18 frames per second throughout testing for optical strain and fiber-alignment analysis.
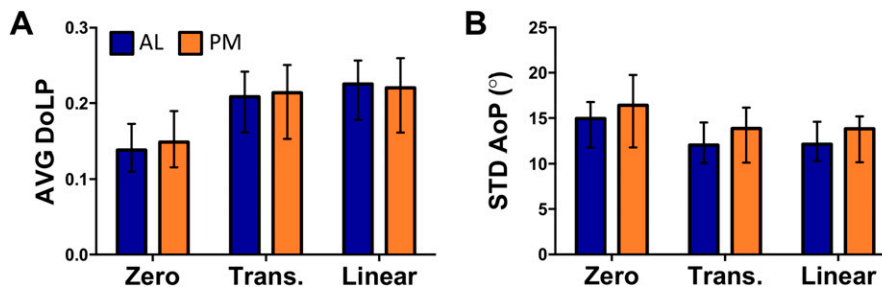

Fig. 4

Microstructural analysis by bundle during the quasi-static ramp-to-failure test. **Fig. 4-A** Mean (AVG) DoLP, with both the anterolateral (AL) and posteromedial (PM) bundles demonstrating increased directional uniformity of collagen alignment with increasing strain. **Fig. 4-B** AoP standard deviation (STD), with both anterolateral and posteromedial bundles demonstrating decreasing variation in alignment with increasing strain. There were no significant inter-bundle differences for these parameters; bars indicate the median, and error bars indicate the 75th and 25th percentiles. Trans. = transition.
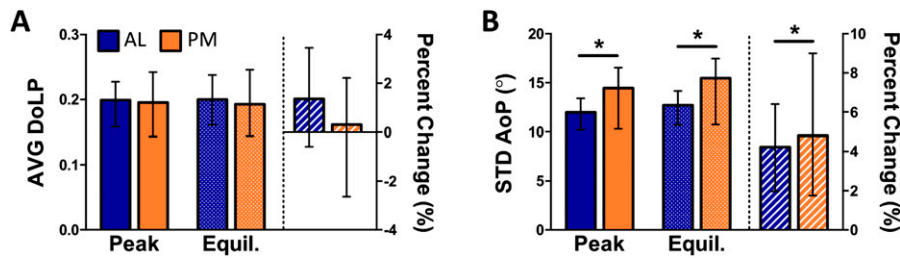
Fig. 5

Microstructural analysis by bundle during the stress-relaxation test. **Fig. 5-A** Mean (AVG) DoLP at peak and equilibrium as well as percent change showed no significant inter-bundle differences. **Fig. 5-B** AoP standard deviation (STD) showed significant inter-bundle differences at both peak and equilibrium points as well as in percent change. The asterisks indicate significance ($p < 0.05$); bars indicate the median, and error bars indicate the 75th and 25th percentiles; AL = anterolateral, PM = posteromedial, and Equil. = equilibrium.

When the circularly polarized light passes through the tissue, the light becomes linearly polarized to some degree in the direction of the collagen fibers in the tissue. This system uses a custom-made division-of-focal-plane polarization imaging camera that can acquire polarization data at high resolution, in real time, to determine the amount (degree of linear polarization [DoLP]) and direction (angle of polarization [AoP]) of polarization after the light passes through the tissue sample[32,34]. The DoLP value corresponds to how much of the light has been polarized by passing through the tissue, and it represents the distribution of collagen fibers (relative degree of isotropy and anisotropy) within each pixel. The AoP value is the average direction of the linear polarization of the light after the light passes through the tissue, and it represents the average direction of collagen alignment contained within each pixel (averaged through the thickness of the sample). Therefore, each pixel has a direction (AoP) and strength (DoLP) of collagen alignment. For
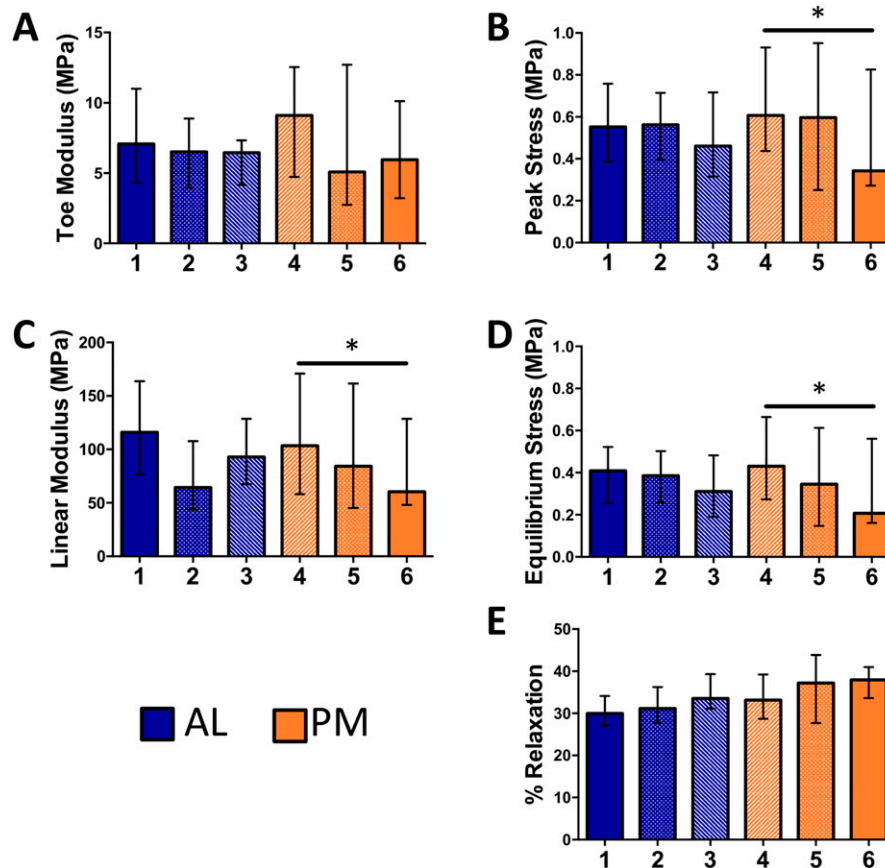
Fig. 6

Mechanical properties by PCL region showing elastic moduli in the toe region (**Fig. 6-A**) and linear region (**Fig. 6-C**) of the stress-strain diagram of the quasi-static ramp-to-failure test as well as peak stress (**Fig. 6-B**), equilibrium stress (**Fig. 6-D**), and percent relaxation from the stress-relaxation test (**Fig. 6-E**). Significant intra-bundle differences were found across the posteromedial bundle (regions 4 to 6) in the elastic modulus and in both peak and equilibrium stress. The asterisks indicate significance ($p < 0.05$); bars indicate the median, and error bars indicate the 75th and 25th percentiles.

Fig. 7

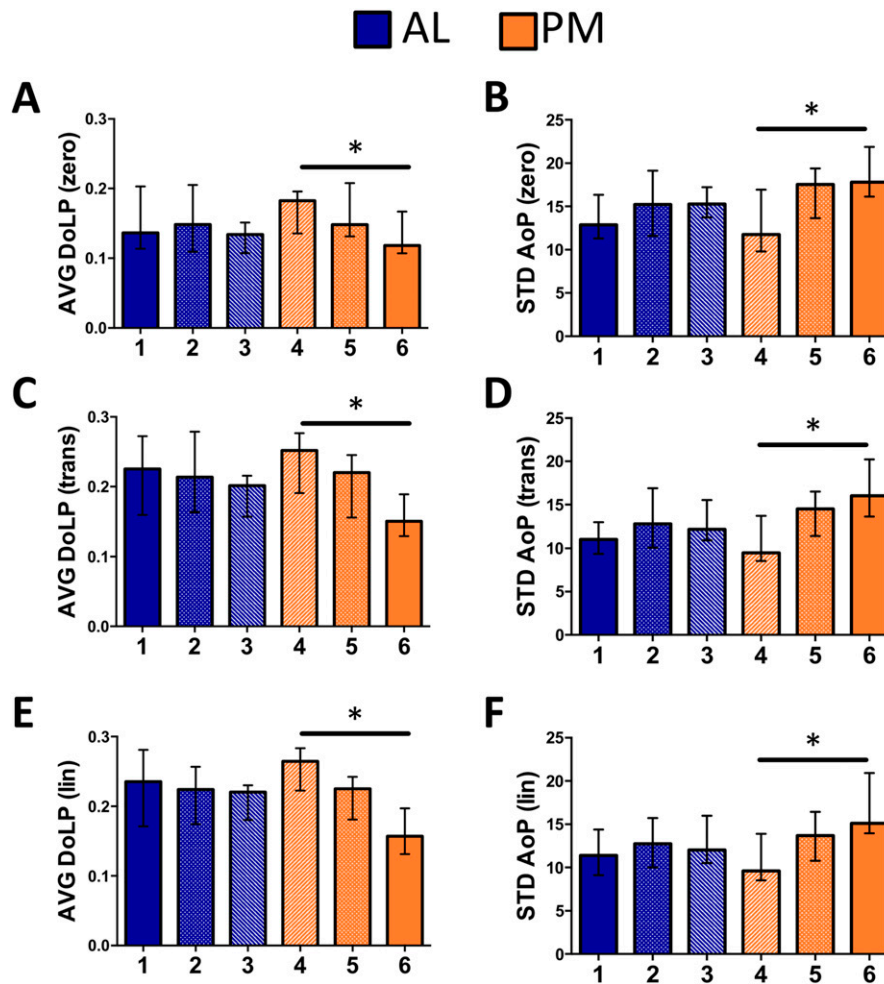Microstructural properties by PCL region during the quasi-static ramp-to-failure test showing mean (AVG) DoLP at zero (**Fig. 7-A**), transition (**Fig. 7-C**), and linear points (**Fig. 7-E**) as well as AoP standard deviation (STD) values at zero (**Fig. 7-B**), transition (**Fig. 7-D**), and linear points (**Fig. 7-F**). All parameters showed significant intra-bundle relationships across the posteromedial bundle (regions 4 to 6), while none reached significance across the anterolateral bundle. The asterisks indicate significance ($p < 0.05$); bars indicate the median, and error bars indicate the 75th and 25th percentiles.

quantitative analysis (Fig. 2), the DoLP and AoP values can be extracted from within a region of interest, defined in this study as the tissue bordered by the 4 brass beads attached to each sample, and they are compared across different groups by calculating the standard deviation of the AoP (representing the degree of variation in orientation angle in each region of interest) and the mean DoLP (representing the mean strength of collagen alignment in each region of interest)[28,29,34,35].

Data and Statistical Analysis

A custom MATLAB program was used to optically track the surface beads and calculate 2-dimensional (2D) Lagrangian strain with use of tensor algebra. Stress was calculated as force divided by the mean initial cross-sectional area of each sample. With use of the least-squares method, a bilinear curve fit was applied to the stress-strain data in order to quantify the elastic modulus in the toe and linear regions as well as the stress and strain values corresponding to the transition point of the bilinear curve fit.

Images corresponding to distinct time points during the stress-relaxation test and quasi-static ramp-to-failure test were selected for analysis. For each image, the mean DoLP and standard deviation of the AoP were calculated in the region of interest defined by the 4 beads. For the quasi-static ramp-to-failure test, these values were then interpolated to calculate alignment parameters corresponding to specific points on the corresponding stress-strain curve, namely zero strain (immediately prior to initiation of the ramp-to-failure test), transition strain (the intersection point of the bilinear curve fit of the stress-strain data), and linear strain (defined as 2 times the transition strain within the linear portion of the stress-strain curve).

With use of Shapiro-Wilk normality tests, the data were determined to be non-normally distributed; therefore, nonparametric statistical analyses were used and the data are presented as the median and interquartile range in each data figure. A linear mixed model was used to identify significant differences between anterolateral and posteromedial bundles with use of JMP software (SAS Institute). This statistical approach accounted for dependence of multiple test samples (6 subsections) taken from each ligament and multiple PCLs (left and right) taken from a given donor. To evaluate variation of properties across the regions of each bundle, linear regression parameters were estimated after appropriately adjusting for the dependencies in the samples (as in the inter-bundle analysis), thus appropriately defining the degrees of freedom for statistical tests. Linear mixed models were fit with use of standard restricted maximum likelihood (REML) estimation procedures, and significance was set at $p < 0.05$.

Results

The anterolateral and posteromedial bundles of the PCL demonstrated similar mechanical and microstructural properties. Elastic moduli calculated during the quasi-static ramp-to-failure test for both toe and linear regions were not significantly different between bundles (Fig. 3-A). In the stress-relaxation test, peak and equilibrium stresses were similar for the anterolateral and posteromedial bundles (Fig. 3-B); however, both percent relaxation and rate of relaxation were found to be significantly different, with more relaxation in the posteromedial than in the anterolateral bundle (p = 0.004; Table II). Based on the time-dependent normalized stress, the inter-bundle difference was significant from the first time point calculated after the ramp through the end of testing (the 5% strain step) (p < 0.05; Fig. 3-C).

During the quasi-static ramp-to-failure test, the mean DoLP increased and the standard deviation of the AoP decreased with increasing strain in both bundles, demonstrating reorganization of collagen fibers under tensile loading. In addition, larger changes occurred from "zero" to "transition" than from "transition" to "linear" in both bundles, indicating that most collagen realignment occurred during the toe-region portion of the stress-strain curve. However, no significant inter-bundle microstructural differences were observed (Fig. 4). Nonetheless, similar to findings with the mechanical properties, significant inter-bundle differences in microstructural properties were observed during the stress-relaxation test (p < 0.05). While the mean DoLP was not different between bundles at peak or equilibrium (Fig. 5-A and Table II), the standard deviation of the AoP was significantly different at both peak (p = 0.018) and equilibrium (p = 0.018), and the percent change of the AoP standard deviation over the hold period also showed significant inter-bundle differences (p = 0.009; Fig. 5-B and Table II).

Although overall properties of the bundles were quite similar, several notable differences were found in intra-bundle comparisons in both mechanical and microstructural properties. Intra-bundle comparisons of mechanical properties of regional samples showed several significant linear relationships across posteromedial regions: linear modulus in the quasi-static ramp-to-failure test (p = 0.042) as well as both peak stress (p = 0.043) and equilibrium stress (p = 0.037) in the stress-relaxation test (Fig. 6 and Table II). All values decreased moving posteriorly. However, no significant intra-bundle relationships were found across anterolateral regions.

Similarly, intra-bundle comparisons of microstructural properties showed significant linear relationships across posteromedial regions (p < 0.05) but not across anterolateral regions (Fig. 7 and Table II). All measured parameters, except percent change of the mean DoLP during the stress-relaxation test, were found to have significant linear regressions across posteromedial regions (p < 0.05 for all and p < 0.001 for most; Table II), with the mean DoLP decreasing and the AoP standard deviation increasing moving posteriorly, a finding consistent with the trend seen in the mechanical properties. Notably, while no regressions reached significance across anterolateral regions, several regressions in both the mean DoLP and the AoP standard deviation trended (p < 0.20) in the same direction as the significant regressions found across posteromedial regions (Table II).

Discussion

The anterolateral and posteromedial bundles of the PCL have very similar microstructural and mechanical properties under tensile loading. These findings are in contrast to previous studies of the ACL[24,28,29,36], including our own[28,29], which found significant regional and bundle variation in the properties of that ligament. The regional variation of these properties in the PCL appears to be much more subtle. Our findings suggest that the distinct functions of the bundles arise more from differences in size and mechanical dynamics due to geometry than from differences in underlying material and microstructural properties.

Values in the literature for mechanical properties of the PCL, based on cadaveric studies with different testing and harvesting techniques, vary greatly[24-27]; this variation makes drawing conclusions about the differences between bundle properties based on tissue-level values alone challenging. An advantage of the present study compared with prior work is that we were able to evaluate the behavior of the collagen microstructure of the ligaments in real time, simultaneously with mechanical testing. Previous studies were unable to simultaneously examine these variables[27,30,37]. The current study provides a more complete picture of ligament behavior and shows only small inter-bundle differences under dynamic loading. Additionally, the mean patient age of samples in this study was much lower than in previous studies, an important distinction since studies have demonstrated that cell proliferation, metabolism, and collagen orientation all decrease with aging[38-40].

Since the anterolateral bundle was traditionally considered the dominant PCL bundle[17,27,41,42], single-bundle techniques for reconstruction historically attempted to recreate this bundle alone. The findings from our study suggest that any so-called dominance of the anterolateral bundle results from greater mass and geometric orientation and location rather than any significant mechanical or microstructural differences between the 2 bundles, in contrast to conclusions of prior studies[17,27]. Moreover, our findings are consistent with recent studies suggesting co-dominance of the PCL bundles[7,43]. These findings may help to explain why smaller case studies have shown that there are similar clinical outcomes between single and double-bundle constructs for PCL reconstruction[44-46] despite biomechanical differences between these constructs[47-52].

The implications for operative treatment of PCL injury are not entirely clear. With only small differences in mechanical and microstructural properties between the bundles, the benefit of the double-bundle technique, if any, likely arises from the use of more tissue and from more closely reapproximating the native ligament geometry, potentially providing more natural kinematics[47-50,53]. In this study, the only parameters that were significantly different between bundles were related to stress-relaxation, namely less relaxation and less dispersed collagen alignment for the anterolateral bundle compared with the posteromedial bundle (Figs. 3 and 5). These results agree with those of our previous studies of ACL bundles and collagen

gel tissue analogs, which showed faster relaxation and greater overall total relaxation for less aligned samples[29,54]. Thus, the PCL bundles exhibit some differences in time-dependent viscoelastic behavior, with a slightly more viscous response for the posteromedial bundle. While it is possible that these differences could have some relevance to injury risk, the clinical implications are not directly obvious because in vivo viscoelasticity will depend on other factors not evaluated in this study, such as physiological water content, anatomical orientation, and degree of prestress in the bundles. In addition, relatively small differences in viscoelastic behavior may not be as clinically important as other parameters measured in this study, such as elastic moduli and stresses.

Similar to the findings of previous studies of the ACL and PCL[29,30], in our study we found that the collagen microstructure within each bundle was not entirely homogenous. Our data show that, at least within the posteromedial bundle, there is a gradient from anterior to posterior in both microstructural and mechanical properties, with collagen in the anterior portion of the bundle more highly aligned and more resistant to tensile forces and with both properties decreasing moving posteriorly. These findings correspond with those of a previous report of increased collagen density in the anterior portions of knee ligaments in general and the ACL bundles in particular[30]. The current study, however, was powered to detect differences between the bundles rather than between regions; therefore, these trends were not fully elucidated, especially in regard to the anterolateral bundle. Further studies would be required in order to fully evaluate intra-bundle variation and whether a linear gradient in the properties of a reconstructed posteromedial bundle could enhance clinical outcomes.

There are a number of limitations to the current study. One important limitation results from anatomical variation. While our study averaged the bundle properties across all of the different anatomical variants, it is possible that material properties may be affected by the variations, especially in light of findings suggesting that the meniscofemoral ligaments, when present, may support the role of the PCL in restraining the knee[55]. Our sample size was not large enough to adequately compare the differences between anatomical variants, and further studies would be needed to fully characterize them. However, we believe this limitation to be of questionable clinical importance, as identifying which anatomic variant a given patient had prior to a PCL injury would likely be impossible unless the patient had had imaging prior to the injury. Also, while dissection was performed systematically to minimize differences between specimens, the anatomical variants invariably resulted in some inter-specimen differences between the sections of the posteromedial bundle, and these were subsequently identified as regions 4, 5, and 6. Finally, in order to prepare samples for testing, multiple freeze-thaw cycles were required. There is the theoretical possibility that freezing may alter the tissue, but previous research has suggested that limited freeze-thaw cycles do not cause meaningful changes in ligamentous tissue properties[56].

Despite these limitations, to our knowledge, this is the first study to report both the microstructural and mechanical properties of the PCL. This ligament has relatively homogenous properties, with only small differences in stress-relaxation behavior between the anterolateral and posteromedial bundles and only subtle regional variation across each bundle. This information may help to guide graft choice and operative techniques for PCL reconstruction. Further research is warranted to assess which techniques and grafts most closely recreate the microstructure of the native PCL as well as to determine the impact of anatomical variation of the ligament, if any, on these findings. ∎

Jon O. Wright, MD[1,2]
Nathan W. Skelley, MD[1]
Reid P. Schur, BS[1]
Ryan M. Castile, BS[1]
Spencer P. Lake, PhD[1]
Robert H. Brophy, MD[1]

[1]Departments of Orthopaedic Surgery (J.O.W., N.W.S., S.P.L, and R.H.B.), Mechanical Engineering and Materials Science (R.P.S., R.M.C., and S.P.L.), and Biomedical Engineering (S.P.L.), Washington University in St. Louis, St. Louis, Missouri

[2]Department of Orthopaedic Surgery, Beaumont Health, Royal Oak, Michigan

E-mail address for R.H. Brophy: brophyr@wudosis.wustl.edu

References

1. Noyes FR, Butler DL, Grood ES, Zernicke RF, Hefzy MS. Biomechanical analysis of human ligament grafts used in knee-ligament repairs and reconstructions. J Bone Joint Surg Am. 1984 Mar;66(3):344-52.

2. Amis AA, Gupte CM, Bull AMJ, Edwards A. Anatomy of the posterior cruciate ligament and the meniscofemoral ligaments. Knee Surg Sports Traumatol Arthrosc. 2006 Mar;14(3):257-63. Epub 2005 Oct 14.

3. Hatsushika D, Nimura A, Mochizuki T, Yamaguchi K, Muneta T, Akita K. Attachments of separate small bundles of human posterior cruciate ligament: an anatomic study. Knee Surg Sports Traumatol Arthrosc. 2013 May;21(5):998-1004. Epub 2012 Sep 29.

4. Chwaluk A, Ciszek B. Anatomy of the posterior cruciate ligament. Ortop Traumatol Rehabil. 2008 Jan-Feb;10(1):1-11.

5. Narvy SJ, Pearl M, Vrla M, Yi A, Hatch GFR 3rd. Anatomy of the femoral footprint of the posterior cruciate ligament: a systematic review. Arthroscopy. 2015 Feb;31(2):345-54. Epub 2014 Sep 4.

6. Edwards A, Bull AMJ, Amis AA. The attachments of the fiber bundles of the posterior cruciate ligament: an anatomic study. Arthroscopy. 2007 Mar;23(3):284-90.

7. Kennedy NI, Wijdicks CA, Goldsmith MT, Michalski MP, Devitt BM, Årøen A, Engebretsen L, LaPrade RF. Kinematic analysis of the posterior cruciate ligament, part 1: the individual and collective function of the anterolateral and posteromedial bundles. Am J Sports Med. 2013 Dec;41(12):2828-38. Epub 2013 Sep 24.

8. Li G, Gill TJ, DeFrate LE, Zayontz S, Glatt V, Zarins B. Biomechanical consequences of PCL deficiency in the knee under simulated muscle loads—an in vitro experimental study. J Orthop Res. 2002 Jul;20(4):887-92.

9. Li G, Papannagari R, Li M, Bingham J, Nha KW, Allred D, Gill T. Effect of posterior cruciate ligament deficiency on in vivo translation and rotation of the knee during weightbearing flexion. Am J Sports Med. 2008 Mar;36(3):474-9. Epub 2007 Dec 5.

MICROSTRUCTURAL AND MECHANICAL PROPERTIES OF THE PCL: A
COMPARISON OF ANTEROLATERAL AND POSTEROMEDIAL BUNDLES

10. Logan M, Williams A, Lavelle J, Gedroyc W, Freeman M. The effect of posterior cruciate ligament deficiency on knee kinematics. Am J Sports Med. 2004 Dec;32 (8):1915-22.

11. Spiridonov SI, Slinkard NJ, LaPrade RF. Isolated and combined grade-III posterior cruciate ligament tears treated with double-bundle reconstruction with use of endoscopically placed femoral tunnels and grafts: operative technique and clinical outcomes. J Bone Joint Surg Am. 2011 Oct 5;93(19):1773-80.

12. Shelbourne KD, Davis TJ, Patel DV. The natural history of acute, isolated, nonoperatively treated posterior cruciate ligament injuries. A prospective study. Am J Sports Med. 1999 May-Jun;27(3):276-83.

13. Parolie JM, Bergfeld JA. Long-term results of nonoperative treatment of isolated posterior cruciate ligament injuries in the athlete. Am J Sports Med. 1986 Jan-Feb;14(1):35-8.

14. Shelbourne KD, Clark M, Gray T. Minimum 10-year follow-up of patients after an acute, isolated posterior cruciate ligament injury treated nonoperatively. Am J Sports Med. 2013 Jul;41(7):1526-33. Epub 2013 May 7.

15. Dandy DJ, Pusey RJ. The long-term results of unrepaired tears of the posterior cruciate ligament. J Bone Joint Surg Br. 1982;64(1):92-4.

16. Patel DV, Allen AA, Warren RF, Wickiewicz TL, Simonian PT. The nonoperative treatment of acute, isolated (partial or complete) posterior cruciate ligament-deficient knees: an intermediate-term follow-up study. HSS J. 2007 Sep;3(2):137-46.

17. Harner CD, Höher J. Evaluation and treatment of posterior cruciate ligament injuries. Am J Sports Med. 1998 May-Jun;26(3):471-82.

18. LaPrade CM, Civitarese DM, Rasmussen MT, LaPrade RF. Emerging updates on the posterior cruciate ligament: a review of the current literature. Am J Sports Med. 2015 Dec;43(12):3077-92. Epub 2015 Mar 16.

19. Del Buono A, Radmilovic J, Gargano G, Gatto S, Maffulli N. Augmentation or reconstruction of PCL? A quantitative review. Knee Surg Sports Traumatol Arthrosc. 2013 May;21(5):1050-63. Epub 2013 Feb 2.

20. Kim YM, Lee CA, Matava MJ. Clinical results of arthroscopic single-bundle transtibial posterior cruciate ligament reconstruction: a systematic review. Am J Sports Med. 2011 Feb;39(2):425-34. Epub 2010 Aug 11.

21. Jung YB, Jung HJ, Song KS, Kim JY, Lee HJ, Lee JS. Remnant posterior cruciate ligament-augmenting stent procedure for injuries in the acute or subacute stage. Arthroscopy. 2010 Feb;26(2):223-9. Epub 2009 Dec 21.

22. Lee KH, Jung YB, Jung HJ, Jang EC, Song KS, Kim JY, Lee SH. Combined posterolateral corner reconstruction with remnant tensioning and augmentation in chronic posterior cruciate ligament injuries: minimum 2-year follow-up. Arthroscopy. 2011 Apr;27(4):507-15.

23. Zhao JZ, Huang-Fu XQ, He YH, Yang XG. Single-bundle posterior cruciate ligament reconstruction with remnant preservation: lateral versus medial-sided augmentation technique. Orthop Surg. 2009 Feb;1(1):66-73.

24. Butler DL, Kay MD, Stouffer DC. Comparison of material properties in fascicle-bone units from human patellar tendon and knee ligaments. J Biomech. 1986;19 (6):425-32.

25. Kennedy JC, Hawkins RJ, Willis RB, Danylchuck KD. Tension studies of human knee ligaments. Yield point, ultimate failure, and disruption of the cruciate and tibial collateral ligaments. J Bone Joint Surg Am. 1976 Apr;58(3):350-5.

26. Marinozzi G, Pappalardo S, Steindler R. Human knee ligaments: mechanical tests and ultrastructural observations. Ital J Orthop Traumatol. 1983 Jun;9(2): 231-40.

27. Race A, Amis AA. The mechanical properties of the two bundles of the human posterior cruciate ligament. J Biomech. 1994 Jan;27(1):13-24.

28. Skelley NW, Castile RM, York TE, Gruev V, Lake SP, Brophy RH. Differences in the microstructural properties of the anteromedial and posterolateral bundles of the anterior cruciate ligament. Am J Sports Med. 2015 Apr;43(4):928-36. Epub 2015 Jan 29.

29. Castile RM, Skelley NW, Babaei B, Brophy RH, Lake SP. Microstructural properties and mechanics vary between bundles of the human anterior cruciate ligament during stress-relaxation. J Biomech. 2016 Jan 4;49(1):87-93. Epub 2015 Nov 22.

30. Mommersteeg TJ, Blankevoort L, Kooloos JG, Hendriks JC, Kauer JM, Huiskes R. Nonuniform distribution of collagen density in human knee ligaments. J Orthop Res. 1994 Mar;12(2):238-45.

31. Anderson CJ, Ziegler CG, Wijdicks CA, Engebretsen L, LaPrade RF. Arthroscopically pertinent anatomy of the anterolateral and posteromedial bundles of the posterior cruciate ligament. J Bone Joint Surg Am. 2012 Nov 7;94(21):1936-45.

32. Gruev V, Perkins R, York T. CCD polarization imaging sensor with aluminum nanowire optical filters. Opt Express. 2010 Aug 30;18(18):19087-94.

33. York T, Gruev V. Characterization of a visible spectrum division-of-focal-plane polarimeter. Appl Opt. 2012 Aug 1;51(22):5392-400.

34. York T, Kahan L, Lake SP, Gruev V. Real-time high-resolution measurement of collagen alignment in dynamically loaded soft tissue. J Biomed Opt. 2014 Jun;19 (6):066011.

35. York T, Powell SB, Gao S, Kahan L, Charanya T, Saha D, Roberts NW, Cronin TW, Marshall J, Achilefu S, Lake SP, Raman B, Gruev V. Bioinspired polarization imaging sensors: from circuits and optics to signal processing algorithms and biomedical applications: analysis at the focal plane emulates nature's method in sensors to image and diagnose with polarized light. Proc IEEE Inst Electr Electron Eng. 2014;102(10):1450-69.

36. Butler DL, Guan Y, Kay MD, Cummings JF, Feder SM, Levy MS. Location-dependent variations in the material properties of the anterior cruciate ligament. J Biomech. 1992 May;25(5):511-8.

37. Amis AA, Bull AMJ, Gupte CM, Hijazi I, Race A, Robinson JR. Biomechanics of the PCL and related structures: posterolateral, posteromedial and meniscofemoral ligaments. Knee Surg Sports Traumatol Arthrosc. 2003 Sep;11(5):271-81. Epub 2003 Sep 5.

38. Hasegawa A, Otsuki S, Pauli C, Miyaki S, Patil S, Steklov N, Kinoshita M, Koziol J, D'Lima DD, Lotz MK. Anterior cruciate ligament changes in the human knee joint in aging and osteoarthritis. Arthritis Rheum. 2012 Mar;64(3):696-704.

39. Levy YD, Hasegawa A, Patil S, Koziol JA, Lotz MK, D'Lima DD. Histopathological changes in the human posterior cruciate ligament during aging and osteoarthritis: correlations with anterior cruciate ligament and cartilage changes. Ann Rheum Dis. 2013 Feb;72(2):271-7. Epub 2012 Aug 7.

40. McCarthy MM, Hannafin JA. The mature athlete: aging tendon and ligament. Sports Health. 2014 Jan;6(1):41-8.

41. Sekiya JK, West RV, Ong BC, Irrgang JJ, Fu FH, Harner CD. Clinical outcomes after isolated arthroscopic single-bundle posterior cruciate ligament reconstruction. Arthroscopy. 2005 Sep;21(9):1042-50.

42. Harner CD, Xerogeanes JW, Livesay GA, Carlin GJ, Smith BA, Kusayama T, Kashiwaguchi S, Woo SL. The human posterior cruciate ligament complex: an interdisciplinary study. Ligament morphology and biomechanical evaluation. Am J Sports Med. 1995 Nov-Dec;23(6):736-45.

43. Ahmad CS, Cohen ZA, Levine WN, Gardner TR, Ateshian GA, Mow VC. Codominance of the individual posterior cruciate ligament bundles. An analysis of bundle lengths and orientation. Am J Sports Med. 2003 Mar-Apr;31(2):221-5.

44. Houe T, Jørgensen U. Arthroscopic posterior cruciate ligament reconstruction: one- vs. two-tunnel technique. Scand J Med Sci Sports. 2004 Apr;14(2):107-11.

45. Wang CJ, Weng LH, Hsu CC, Chan YS. Arthroscopic single- versus double-bundle posterior cruciate ligament reconstructions using hamstring autograft. Injury. 2004 Dec;35(12):1293-9.

46. Kohen RB, Sekiya JK. Single-bundle versus double-bundle posterior cruciate ligament reconstruction. Arthroscopy. 2009 Dec;25(12):1470-7. Epub 2009 Jan 24.

47. Wijdicks CA, Kennedy NI, Goldsmith MT, Devitt BM, Michalski MP, Årøen A, Engebretsen L, LaPrade RF. Kinematic analysis of the posterior cruciate ligament, part 2: a comparison of anatomic single- versus double-bundle reconstruction. Am J Sports Med. 2013 Dec;41(12):2839-48. Epub 2013 Oct 3.

48. Race A, Amis AA. PCL reconstruction. In vitro biomechanical comparison of 'isometric' versus single and double-bundled 'anatomic' grafts. J Bone Joint Surg Br. 1998 Jan;80(1):173-9.

49. Kim SJ, Kim SH, Kim SG, Kung YP. Comparison of the clinical results of three posterior cruciate ligament reconstruction techniques: surgical technique. J Bone Joint Surg Am. 2010 Sep;92(Suppl 1 Pt 2):145-57.

50. Harner CD, Janaushek MA, Kanamori A, Yagi M, Vogrin TM, Woo SL. Biomechanical analysis of a double-bundle posterior cruciate ligament reconstruction. Am J Sports Med. 2000 Mar-Apr;28(2):144-51.

51. Kennedy NI, LaPrade RF, Goldsmith MT, Faucett SC, Rasmussen MT, Coatney GA, Engebretsen L, Wijdicks CA. Posterior cruciate ligament graft fixation angles, part 1: biomechanical evaluation for anatomic single-bundle reconstruction. Am J Sports Med. 2014 Oct;42(10):2338-45. Epub 2014 Aug 4.

52. Kennedy NI, LaPrade RF, Goldsmith MT, Faucett SC, Rasmussen MT, Coatney GA, Engebretsen L, Wijdicks CA. Posterior cruciate ligament graft fixation angles, part 2: biomechanical evaluation for anatomic double-bundle reconstruction. Am J Sports Med. 2014 Oct;42(10):2346-55. Epub 2014 Aug 4.

53. Tsukada H, Ishibashi Y, Tsuda E, Fukuda A, Yamamoto Y, Toh S. Biomechanical evaluation of an anatomic double-bundle posterior cruciate ligament reconstruction. Arthroscopy. 2012 Feb;28(2):264-71. Epub 2011 Oct 22.

54. Lake SP, Barocas VH. Mechanics and kinematics of soft tissue under indentation are determined by the degree of initial collagen fiber alignment. J Mech Behav Biomed Mater. 2012 Sep;13:25-35. Epub 2012 May 14.

55. Lertwanich P, Martins CAQ, Kato Y, Ingham SJ, Kramer S, Linde-Rosen M, Smolinski P, Fu FH. Contribution of the meniscofemoral ligament as a restraint to the posterior tibial translation in a porcine knee. Knee Surg Sports Traumatol Arthrosc. 2010 Sep;18(9):1277-81. Epub 2010 Apr 21.

56. Woo SL, Orlando CA, Camp JF, Akeson WH. Effects of postmortem storage by freezing on ligament tensile behavior. J Biomech. 1986;19(5):399-404.